ROZPRAWY INŻYNIERSKIE • ENGINEERING TRANSACTIONS • 27, 1, 53—68, 1979
Polska Akademia Nauk • Instytut Podstawowych Problemów Techniki

THE POST-BUCKLING STATE OF A MULTILAYERED SHELL IN A FORM OF A CYLINDER SECTOR SUBJECTED TO AN UNIDIRECTIONAL COMPRESSION AND SIMULTANEOUS SHEAR

W. WALCZAK AND N. X. LUU (ŁÓDŹ)

In the paper are presented the results of theoretical analysis of post-buckling state of a thin-walled, elastic, multilayered shell in a form of a cylindrical sector, subjected to the action of unidirectional compression and simultaneous shear. The shell consists of orthotropic layers and has a symmetric structure. The problem is solved approximately on the basis of the non-linear version of the anisotropic shell theory given by S. A. Ambarcumian. The detailed numerical computations are made for a shell consisting of five orthotropic layers, and results of these computations are presented in the form of diagrams. The numerical computations were made on the ODRA-1204 computer.

1. INTRODUCTION

Load-carrying elements of many contemporary engineering constructions are made in the form of thin-walled shells. Very often these shells are shaped like cylinder sectors and are built as multilayered constructions consisting of anisotropic or orthotropic layers.

Shells, as load-carrying elements, generally work in a composed loading state. Often, at short-lived overcharges, values of these loadings exceed the critical values. In this regard the knowledge of the behaviour of shells in post-buckling states, in particular at composed loadings, is now of great significance both cognitive and practical.

The bases of the theory of multilayered shells consisting of anisotropic layers are given by S. A. AMBARCUMIAN [1]. Nonlinear differential equations describing multilayered shallow cylinder shells are presented, among others, by E. I. GRIGOLYUK and P. P. CHULKOV [3]. Many authors, including L. M. KURSHIN [4], O. N. LENKO [5] and W. SZYC [6], investigated in a nonlinear conception the stability problem of three-layered cylinder shells at different loadings. T. NIEZGODZIŃSKI [7] analysed the stability and the post-buckling state of a multilayered shell in a form of a cylinder sector subjected to shear.

This paper presents a solution to the problem of nonlinear stability of a multilayered shell having the form of a cylinder sector under shear and simultaneous unidirectional compression along cylinder generating lines. This problem has been solved in an approximate manner.

2. Assumptions and governing differential equations

The subject of our considerations is a multilayered shell at a little shallowness in the form of a cylinder sector with a radius R, consisting of homogeneous orthotropic layers. The constant whole thickness is h and the length of the edges of the considered shell are a and b.

It has been assumed that the shell is simply supported along its perimeter and subjected to an action of compression loadings p and shear loadings s — per unit of edge length of the shell (Fig. 1).

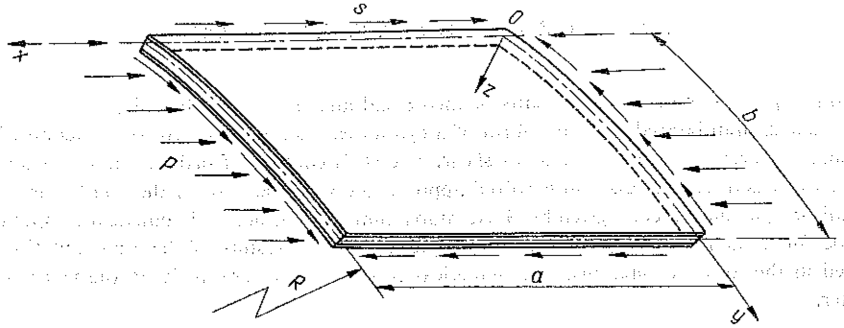

FIG. 1.

In practical solutions of engineering constructions, the multilayered shells having a symmetric structure are the most often applied. The cross-section of a shell built from $(2m+1)$ layers — symmetrically located about the coordinates surface x, y — is shown in Fig. 2.

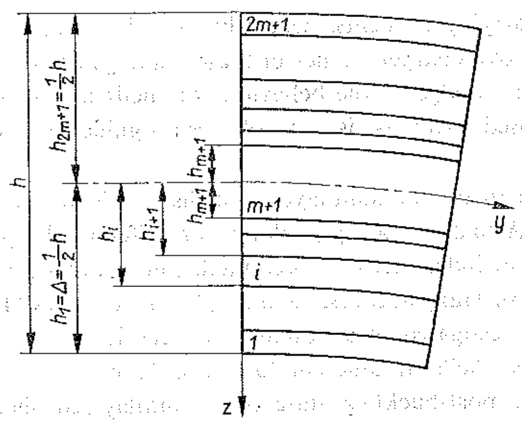

FIG. 2.

The problem has been considered on the basis of the nonlinear version of the theory of anisotropic shells given by S. A. AMBARCUMIAN [1]. In the case of a multilayered anisotropic shell the sectional forces acting on the edges of any shell element

(Fig. 3) are expressed, in terms of linear functions of strain state components, as follows [1]:

$$
\begin{aligned}
&N_x = C_{11}\varepsilon_1 + C_{12}\varepsilon_2 + C_{16}\gamma_0,\\
&N_y = C_{12}\varepsilon_1 + C_{22}\varepsilon_2 + C_{26}\gamma_0,\\
&T_{xy} = T_{yx} = T = C_{16}\varepsilon_1 + C_{26}\varepsilon_2 + C_{66}\gamma_0,\\
&M_x = D_{11}\kappa_1 + D_{12}\kappa_2 + D_{16}\chi,\\
&M_y = D_{12}\kappa_1 + D_{22}\kappa_2 + D_{26}\chi,\\
&M_{xy} = M_{yx} = H = D_{16}\kappa_1 + D_{26}\kappa_2 + D_{66}\chi.
\end{aligned}
\tag{2.1}
$$

In the above formulae ε_1, ε_2, and γ_0 denote the strain state components of points of the coordinates surface x, y expressed as functions of the displacement state components u, v and w, appearing in the directions x, y and z, respectively, of the

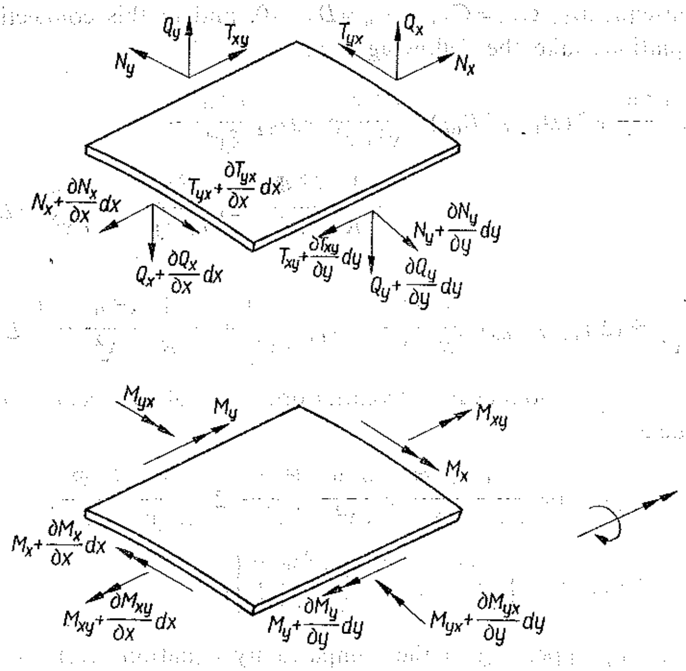

FIG. 3.

accepted system of coordinates. However, changes of the curvatures κ_1 and κ_2, respectively in the directions x and y, and of torsion χ of the coordinates surface are dependent only on the component w [2]. The coefficients C_{jk} and D_{jk} are adequate rigidities of a multilayered shell. If the shell is built from $(2m+1)$ layers (Fig. 2,) symmetrically distributed with respect to the coordinates surface x, y, the rigidity coefficients C_{jk} and D_{jk} are determined by the formulae:

$$(2.2)\qquad \begin{aligned} C_{jk} &= 2\left[B_{jk}^{m+1} h_{m+1} + \sum_{i=1}^{m} B_{jk}^{i} (h_i - h_{i+1})\right], \\ D_{jk} &= \frac{2}{3}\left[B_{jk}^{m+1} h_{m+1}^3 + \sum_{i=1}^{m} B_{jk}^{i} (h_i^3 - h_{i+1}^3)\right], \end{aligned}$$

where B_{jk}^{i} constant depends on the material properties of any i-th layer of shell.

The nonlinear theory of thin-walled anisotropic shells at a little shallowness provided two governing differential equations consisting of two unknown functions: the deflection function $w = w(x, y)$ and the stress function $\Phi = \Phi(x, y)$.

For the considered multilayered shell of a symmetrical structure, consisting of orthotropic layers, it was also assumed that the main directions of orthotropy are parallel to the axes x and y of the accepted coordinates system. In this case the coefficients B_{16} and B_{26} which are dependent on material properties are equal to zero and, consequently, $C_{16} = C_{26} = D_{16} = D_{26} = 0$, and in this connection the two governing equations take the following form:

$$(2.3)\qquad D_{11}\frac{\partial^4 w}{\partial x^4} + 2(D_{12} + 2D_{66})\frac{\partial^4 w}{\partial x^2 \partial y^2} + D_{22}\frac{\partial^4 w}{\partial y^4} - \\ - \frac{1}{R}\frac{\partial^2 \Phi}{\partial x^2} - 2s\frac{\partial^2 w}{\partial x \partial y} + p\frac{\partial^2 w}{\partial x^2} - L(w, \Phi) = 0,$$

and

$$(2.4)\qquad A_{22}\frac{\partial^4 \Phi}{\partial x^4} + (2A_{12} + A_{66})\frac{\partial^4 \Phi}{\partial x^2 \partial y^2} + A_{11}\frac{\partial^4 \Phi}{\partial y^4} = -\frac{1}{R}\frac{\partial^2 w}{\partial x^2} - \frac{1}{2}L(w, w),$$

where $L(..., ...)$ are the nonlinear differential operators of the second order defined by the formulae

$$(2.5)\qquad \begin{aligned} L(w, \Phi) &= \frac{\partial^2 w}{\partial x^2}\frac{\partial^2 \Phi}{\partial y^2} + \frac{\partial^2 w}{\partial y^2}\frac{\partial^2 \Phi}{\partial x^2} - 2\frac{\partial^2 w}{\partial x \partial y}\frac{\partial^2 \Phi}{\partial x \partial y}, \\ L(w, w) &= 2\left[\frac{\partial^2 w}{\partial x^2}\frac{\partial^2 w}{\partial y^2} - \left(\frac{\partial^2 w}{\partial x \partial y}\right)^2\right]. \end{aligned}$$

The coefficients A_{jk} appearing in the compatibility equation (2.4) are determined as follows:

$$(2.6)\qquad \begin{aligned} A_{11} &= \frac{C_{22} C_{66}}{\Omega}, \quad & A_{12} &= -\frac{C_{12} C_{66}}{\Omega}, \\ A_{22} &= \frac{C_{11} C_{66}}{\Omega}, \quad & A_{66} &= \frac{C_{11} C_{22} - (C_{12})^2}{\Omega}, \end{aligned}$$

where

$$(2.7)\qquad \Omega = C_{66}\left[C_{11} C_{22} - (C_{12})^2\right].$$

3. The approximate solution of problem

In order to get an approximate solution of the tittle problem, the following approximate form of the deflection function is assumed:

$$w=f_{11}\sin\frac{\pi x}{a}\sin\frac{\pi y}{b}+f_{12}\sin\frac{\pi x}{a}\sin\frac{2\pi y}{b}+ +f_{21}\sin\frac{2\pi x}{a}\sin\frac{\pi y}{b}+f_{22}\sin\frac{2\pi x}{a}\sin\frac{2\pi y}{b}, \tag{3.1}$$

in which the coefficients f_{11}, f_{12}, f_{21} and f_{22} are independent parameters of a normal shell deflection.

The assumed expression for the deflection function satisfies the boundary conditions for simply supported edges of the shell. Namely, it becomes

$$\begin{aligned} [w]_{\substack{x=0\\x=a}}&=0, & [w]_{\substack{y=0\\y=b}}&=0,\\ [M_x]_{\substack{x=0\\x=a}}&=0, & [M_y]_{\substack{y=0\\y=b}}&=0. \end{aligned} \tag{3.2}$$

In order to determine the stress function $\Phi=\Phi(x,y)$, the compatibility equation (2.4) is availed of. For this purpose the deflection function (3.1) was introduced into the right side of this equation. After differentiation the whole expression was presented as a sum of cosines. The stress function Φ is accepted in the same form as that of the right side of Eq. (2.4), namely

$$\begin{aligned} \Phi=&\Phi_1\cos\alpha+\Phi_2\cos\beta+\Phi_3\cos2\alpha+\Phi_4\cos2\beta+\Phi_5\cos3\alpha+\Phi_6\cos3\beta+\\ &+\Phi_7\cos4\alpha+\Phi_8\cos4\beta+\Phi_9\cos(\alpha+\beta)+\Phi_{10}\cos(\alpha-\beta)+\\ &+\Phi_{11}\cos(2\alpha+2\beta)+ +\Phi_{12}\cos(2\alpha-2\beta)+\Phi_{13}\cos(\alpha+2\beta)+\\ &+\Phi_{14}\cos(\alpha-2\beta)+\Phi_{15}\cos(2\alpha+\beta)+\Phi_{16}\cos(2\alpha-\beta)+\\ &+\Phi_{17}\cos(\alpha+3\beta)+\Phi_{18}\cos(\alpha-3\beta)+\Phi_{19}\cos(3\alpha+\beta)+\\ &+\Phi_{20}\cos(3\alpha-\beta)+\Phi_{21}\cos(\alpha+4\beta)+\Phi_{22}\cos(\alpha-4\beta)+\\ &+\Phi_{23}\cos(4\alpha+\beta)+\Phi_{24}\cos(4\alpha-\beta)+\Phi_{25}\cos(2\alpha+3\beta)+\\ &+\Phi_{26}\cos(2\alpha-3\beta)+\Phi_{27}\cos(3\alpha+2\beta)+\Phi_{28}\cos(3\alpha-2\beta)+\\ &+\Phi_{29}\cos(3\alpha+3\beta)+\Phi_{30}\cos(3\alpha-3\beta)+\Phi_{31}\cos(3\alpha+4\beta)+\\ &+\Phi_{32}\cos(3\alpha-4\beta)+\Phi_{33}\cos(4\alpha+3\beta)+\Phi_{34}\cos(4\alpha-3\beta). \end{aligned} \tag{3.3}$$

In the above expression the unknown coefficients were marked by the symbols $\Phi_1, \Phi_2, \ldots, \Phi_{34}$, and for simplification of the notes the following determinations were introduced:

$$\alpha=\frac{\pi x}{a} \quad \text{and} \quad \beta=\frac{\pi y}{b}. \tag{3.4}$$

The coefficients $\Phi_1, \Phi_2, \ldots, \Phi_{34}$ were determined by comparing the terms standing for the same functions on the left and on the right sides of the compatibility equation (2.4). Hence

(3.5)
$$
\begin{aligned}
\Phi_1 &= -(f_{11}f_{21}+4f_{22}f_{12})\frac{1}{4A_{22}}\left(\frac{a}{b}\right)^2,\\
\Phi_2 &= -(f_{11}f_{12}+4f_{22}f_{21})\frac{1}{4A_{11}}\left(\frac{b}{a}\right)^2,\\
\Phi_3 &= (f_{11}^2+4f_{12}^2)\frac{1}{32A_{22}}\left(\frac{a}{b}\right)^2,\\
\Phi_4 &= (f_{11}^2+4f_{21}^2)\frac{1}{32A_{11}}\left(\frac{b}{a}\right)^2,\\
\Phi_5 &= (f_{11}f_{21}+4f_{22}f_{12})\frac{1}{36A_{22}}\left(\frac{a}{b}\right)^2,\\
\Phi_6 &= (f_{11}f_{12}+4f_{22}f_{21})\frac{1}{36A_{11}}\left(\frac{b}{a}\right)^2,\\
\Phi_7 &= (f_{21}^2+4f_{22}^2)\frac{1}{128A_{22}}\left(\frac{a}{b}\right)^2,\\
\Phi_8 &= (f_{12}^2+4f_{22}^2)\frac{1}{128A_{11}}\left(\frac{b}{a}\right)^2,\\
\Phi_9 &= -\left(9f_{12}f_{21}+\frac{4b^2}{\pi^2 R}f_{11}\right)\frac{1}{8a^2b^2\eta_1},\\
\Phi_{10} &= -\left(9f_{12}f_{21}-\frac{4b^2}{\pi^2 R}f_{11}\right)\frac{1}{8a^2b^2\eta_1},\\
\Phi_{11} &= -\Phi_{12} = -f_{22}\frac{1}{8\pi^2 Ra^2\eta_1},\\
\Phi_{13} &= \left(9f_{11}f_{21}-\frac{4b^2}{\pi^2 R}f_{12}\right)\frac{1}{8a^2b^2\eta_2},\\
\Phi_{14} &= \left(9f_{11}f_{21}+\frac{4b^2}{\pi^2 R}f_{12}\right)\frac{1}{8a^2b^2\eta_2},\\
\Phi_{15} &= \left(9f_{11}f_{21}-\frac{16b^2}{\pi^2 R}f_{21}\right)\frac{1}{8a^2b^2\eta_3},\\
\Phi_{16} &= \left(9f_{11}f_{12}+\frac{16b^2}{\pi^2 R}f_{21}\right)\frac{1}{8a^2b^2\eta_3},\\
\Phi_{17} &= \Phi_{18} = (16f_{11}f_{22}+25f_{12}f_{21})\frac{1}{8a^2b^2\eta_4},\\
\Phi_{19} &= \Phi_{20} = (16f_{11}f_{22}+25f_{12}f_{21})\frac{1}{8a^2b^2\eta_5},
\end{aligned}
$$

(3.5) [cont]

$$\Phi_{21}=\Phi_{22}=f_{22}f_{12}\frac{9}{8a^2b^2\eta_6},$$

$$\Phi_{23}=\Phi_{24}=f_{22}f_{21}\frac{9}{2a^2b^2\eta_7},$$

$$\Phi_{25}=\Phi_{26}=-f_{11}f_{12}\frac{1}{8a^2b^2\eta_8},$$

$$\Phi_{27}=\Phi_{28}=-f_{11}f_{21}\frac{1}{8a^2b^2\eta_9},$$

$$\Phi_{29}=\Phi_{30}=-f_{12}f_{21}\frac{1}{72a^2b^2\eta_1},$$

$$\Phi_{31}=\Phi_{32}=-f_{22}f_{12}\frac{1}{2a^2b^2\eta_{10}},$$

$$\Phi_{33}=\Phi_{34}=-f_{22}f_{21}\frac{1}{2a^2b^2\eta_{11}}.$$

In the above expressions the following determinations were introduced:

(3.6)

$$\eta_1=A_{22}\frac{1}{a^4}+(2A_{12}+A_{66})\frac{1}{a^2b^2}+A_{11}\frac{1}{b^4},$$

$$\eta_2=A_{22}\frac{1}{a^4}+(2A_{12}+A_{66})\frac{4}{a^2b^2}+A_{11}\frac{16}{b^4},$$

$$\eta_3=A_{22}\frac{16}{a^4}+(2A_{12}+A_{66})\frac{4}{a^2b^2}+A_{11}\frac{1}{b^4},$$

$$\eta_4=A_{22}\frac{1}{a^4}+(2A_{12}+A_{66})\frac{9}{a^2b^2}+A_{11}\frac{81}{b^4},$$

$$\eta_5=A_{22}\frac{81}{a^4}+(2A_{12}+A_{66})\frac{9}{a^2b^2}+A_{11}\frac{1}{b^4},$$

$$\eta_6=A_{22}\frac{1}{a^4}+(2A_{12}+A_{66})\frac{16}{a^2b^2}+A_{11}\frac{256}{b^4},$$

$$\eta_7=A_{22}\frac{256}{a^4}+(2A_{12}+A_{66})\frac{16}{a^2b^2}+A_{11}\frac{1}{b^4},$$

$$\eta_8=A_{22}\frac{16}{a^4}+(2A_{12}+A_{66})\frac{36}{a^2b^2}+A_{11}\frac{81}{b^4},$$

$$\eta_9=A_{22}\frac{81}{a^4}+(2A_{12}+A_{66})\frac{36}{a^2b^2}+A_{11}\frac{16}{b^4},$$

$$\eta_{10}=A_{22}\frac{81}{a^4}+(2A_{12}+A_{66})\frac{144}{a^2b^2}+A_{11}\frac{256}{b^4},$$

$$\eta_{11}=A_{22}\frac{256}{a^4}+(2A_{12}+A_{66})\frac{144}{a^2b^2}+A_{11}\frac{256}{b^4}.$$

In order to determine the unknown coefficients f_{11}, f_{12}, f_{21} and f_{22} appearing in the assumed deflection function $w=w(x, y)$, the equilibrium equation (2.3) is used. For solving this equation the Bubnov-Galerkin's method was applied. In the case considered the following system of four equations has an application:

$$
\begin{aligned}
&\int_0^a\int_0^b X\sin\frac{\pi x}{a}\sin\frac{\pi y}{b}\,dx\,dy=0, \qquad \int_0^a\int_0^b X\sin\frac{\pi x}{a}\sin\frac{2\pi y}{b}\,dx\,dy=0,\\
&\int_0^a\int_0^b X\sin\frac{2\pi x}{a}\sin\frac{\pi y}{b}\,dx\,dy=0, \qquad \int_0^a\int_0^b X\sin\frac{2\pi x}{a}\sin\frac{2\pi y}{b}\,dx\,dy=0.
\end{aligned}
\tag{3.7}
$$

In these equations the left side of Eq. (2.3) is determined using the symbol X.

In further considerations the following dimensionless coefficients are introduced: the outside loading coefficient of shell edges:

$$s^*=\frac{ab}{Eh^3}s \quad\text{and}\quad p^*=\frac{b^2}{Eh^3}p, \tag{3.8}$$

the coefficients of a shell form and of a shell shallowness:

$$\lambda=\frac{a}{b} \quad\text{and}\quad k=\frac{b^2}{Rh}, \tag{3.9}$$

the coefficients of a shell deflection:

$$\xi=\frac{f_{11}}{h}, \quad \Psi=\frac{f_{22}}{f_{11}}, \quad \varphi=\frac{f_{12}}{f_{11}}, \quad \theta=\frac{f_{21}}{f_{11}}, \tag{3.10}$$

the coefficients

$$
\begin{aligned}
&\vartheta_i=E_i\,a^2b^2h\eta_i,\\
&\bar{A}_{11}=A_{11}Eh, \quad \bar{A}_{22}=A_{22}Eh,\\
&L_1=\frac{a^2b^2}{Eh^3}\left[D_{11}\frac{1}{a^4}+(D_{12}+2D_{66})\frac{2}{a^2b^2}+D_{22}\frac{1}{b^4}\right],\\
&L_2=\frac{a^2b^2}{Eh^3}\left[D_{11}\frac{1}{a^4}+(D_{12}+2D_{66})\frac{8}{a^2b^2}+D_{22}\frac{16}{b^4}\right],\\
&L_3=\frac{a^2b^2}{Eh^3}\left[D_{11}\frac{16}{a^4}+(D_{12}+2D_{66})\frac{8}{a^2b^2}+D_{22}\frac{1}{b^4}\right],
\end{aligned}
\tag{3.11}
$$

where E is Young's modulus.

Performing integration in the formulae (3.7) and introducing the above given dimensionless coefficients, the following system of four nonlinear algebraical equations is obtained:

$$\varphi\theta\Psi\xi^2\pi^2\left(\frac{1}{\bar{A}_{11}\lambda^2}+\frac{\lambda^2}{\bar{A}_{22}}+\frac{25}{\vartheta_4}+\frac{25}{\vartheta_5}\right)+ \tag{3.12}$$

(3.12) [cont.]
$$+\varphi^2\xi^2\frac{\pi^2}{4}\left(\frac{1}{\bar{A}_{11}\lambda^2}+\frac{\lambda^2}{\bar{A}_{22}}+\frac{81}{4\vartheta_3}+\frac{1}{4\vartheta_8}\right)+\theta^2\xi^2\frac{\pi^2}{4}\left(\frac{1}{\bar{A}_{11}\lambda^2}+\frac{\lambda^2}{\bar{A}_{22}}+\frac{81}{4\vartheta_2}+\frac{1}{4\vartheta_9}\right)+\Psi^2\xi^2 16\pi^2\left(\frac{1}{\vartheta_4}+\frac{1}{\vartheta_5}\right)+\xi^2\frac{\pi^2}{16}\left(\frac{1}{\bar{A}_{11}\lambda^2}+\frac{\lambda^2}{\bar{A}_{22}}\right)-$$
$$-\theta^2\xi\frac{2k}{15\pi^2}\left(\frac{\lambda^2}{\bar{A}_{22}}+\frac{768}{\vartheta_3}\right)-\varphi^2\xi\frac{8k}{3\pi^2}\left(\frac{\lambda^2}{\bar{A}_{22}}+\frac{48}{5\vartheta_2}\right)-$$
$$-\Psi^2\xi\frac{8k}{15\pi^2}\left(\frac{\lambda^2}{\bar{A}_{22}}+\frac{16}{\vartheta_1}\right)-\xi\frac{2k}{3\pi^2}\left(\frac{\lambda^2}{\bar{A}_{22}}+\frac{16}{\vartheta_1}\right)-\frac{128}{9\pi^2}\Psi s^*+$$
$$+\pi^2 L_1+\frac{k^2}{\pi^2\vartheta_1}-p^*=0;$$

(3.13)
$$\varphi^3\xi^2\frac{\pi^2}{16}\left(\frac{1}{\bar{A}_{11}\lambda^2}+\frac{16\lambda^2}{\bar{A}_{22}}\right)+\Psi^2\varphi\xi^2\pi^2\frac{\pi^2}{4}+\left(\frac{1}{\bar{A}_{11}\lambda^2}+\frac{16\lambda^2}{\bar{A}_{22}}+\frac{324}{\vartheta_6}+\frac{4}{\vartheta_{10}}\right)+\theta\Psi\xi^2\pi^2\left(\frac{1}{\bar{A}_{11}\lambda^2}+\frac{\lambda^2}{\bar{A}_{22}}+\frac{25}{\vartheta_4}+\frac{25}{\vartheta_5}\right)+$$
$$+\varphi\xi^2\frac{\pi^2}{4}\left(\frac{1}{\bar{A}_{11}\lambda^2}+\frac{\lambda^2}{\bar{A}_{22}}+\frac{81}{4\vartheta_3}+\frac{1}{4\vartheta_8}\right)+\varphi\theta^2\xi\frac{\pi^2}{16}\times$$
$$\times\left(\frac{82}{\vartheta_1}+\frac{625}{\vartheta_4}+\frac{625}{\vartheta_5}\right)-\theta\Psi\xi\frac{128k}{75\pi^2}\left(\frac{11}{\vartheta_1}+\frac{176}{\vartheta_3}+\frac{60}{\vartheta_7}+\frac{4}{\vartheta_{11}}\right)-$$
$$-\frac{32k}{\pi^2}\varphi\xi\left(\frac{4}{5\vartheta_2}+\frac{4}{5\vartheta_1}+\frac{1}{\vartheta_3}+\frac{1}{15\vartheta_8}\right)+$$
$$+\varphi\left(\pi^2 L_2+\frac{k^2}{\pi^2\vartheta_2}-p^*\right)+\frac{128}{9\pi^2}\theta s^*=0;$$

(3.14)
$$\theta^3\xi^2\frac{\pi^2}{16}\left(\frac{16}{\bar{A}_{11}\lambda^2}+\frac{\lambda^2}{\bar{A}_{22}}\right)+\varphi^2\theta\xi^2\frac{\pi^2}{16}\left(\frac{82}{\vartheta_1}+\frac{625}{\vartheta_4}+\frac{625}{\vartheta_5}\right)+$$
$$+\Psi^2\theta\xi^2\frac{\pi^2}{4}\left(\frac{16}{\bar{A}_{11}\lambda^2}+\frac{\lambda^2}{\bar{A}_{22}}+\frac{324}{\vartheta_7}+\frac{4}{\vartheta_{11}}\right)+\varphi\Psi\xi^2\pi^2\times$$
$$\times\left(\frac{1}{\bar{A}_{11}\lambda^2}+\frac{\lambda^2}{\bar{A}_{22}}+\frac{25}{\vartheta_4}+\frac{25}{\vartheta_5}\right)+\theta\xi^2\frac{\pi^2}{4}\left(\frac{1}{\bar{A}_{11}\lambda^2}+\frac{\lambda^2}{\bar{A}_{22}}+\frac{81}{4\vartheta_2}+\frac{1}{4\vartheta_9}\right)-\varphi\Psi\xi\frac{128k}{5\pi^2}\left(\frac{2\lambda^2}{3\bar{A}_{22}}+\frac{11}{15\vartheta_1}+\frac{44}{15\vartheta_2}+\frac{1}{4\vartheta_6}+\frac{2}{30\vartheta_{10}}\right)-\theta\xi\frac{64k}{15\pi^2}\left(\frac{\lambda^2}{\bar{A}_{22}}+\frac{6}{\vartheta_1}+\frac{15}{8\vartheta_2}+\frac{24}{\vartheta_3}+\frac{9}{8\vartheta_9}\right)+$$
$$+\theta\left(\pi^2 L_3+\frac{16k^2}{\pi^2\vartheta_3}-4p^*\right)+\frac{128}{9\pi^2}\varphi s^*=0;$$

$$
\begin{aligned}
(3.15)\qquad & \Psi^3\xi^2\pi^2\left(\frac{1}{\bar{A}_{11}\lambda^2}+\frac{\lambda^2}{\bar{A}_{22}}\right)+\varphi^2\Psi\xi^2\frac{\pi^2}{4}\left(\frac{1}{\bar{A}_{11}\lambda^2}+\frac{16\lambda^2}{\bar{A}_{22}}+\frac{324}{\vartheta_6}+\frac{4}{\vartheta_{10}}\right)+\\
&+\theta^2\Psi\xi\frac{\pi^2}{4}\left(\frac{16}{\bar{A}_{11}\lambda^2}+\frac{\lambda^2}{\bar{A}_{22}}+\frac{324}{\vartheta_7}+\frac{4}{\vartheta_{11}}\right)+\varphi\theta\xi^2\pi^2\left(\frac{1}{\bar{A}_{11}\lambda^2}+\frac{\lambda^2}{\bar{A}_{22}}+\right.\\
&\left.+\frac{25}{\vartheta_4}+\frac{25}{\vartheta_5}\right)+\Psi\xi^2 16\pi^2\left(\frac{1}{\vartheta_4}+\frac{1}{\vartheta_5}\right)-\frac{16k}{\pi^2}\varphi\theta\xi\left(\frac{26}{15\vartheta_1}+\frac{1024}{225\vartheta_2}+\right.\\
&\left.+\frac{1408}{75\vartheta_3}+\frac{5}{3\vartheta_4}+\frac{15}{\vartheta_5}\right)-\frac{128k}{3\pi^2}\Psi\xi\left(\frac{1}{\vartheta_1}+\frac{2}{5\vartheta_4}+\frac{18}{5\vartheta_5}\right)+\\
&+\Psi\left(16\pi^2 L_1+\frac{k^2}{\pi^2\vartheta_1}-4p^*\right)-\frac{128}{9\pi^2}s^*=0.
\end{aligned}
$$

The system of the above equations is solved in such a manner that the dimensionless coefficient of the uniform compressive loading p^* is treated as a constant parameter, and the dimensionless coefficient of the shell deflection ξ — as a variable parameter. The other dimensionless coefficients Ψ, φ, θ and s^* are functions of the coefficient ξ. By eliminating the dimensionless coefficients Ψ, φ and θ from the above equations, it is possible to find values of the dimensionless coefficient s^* of the shell shear loading as a function of the coefficient ξ by the given dimensionless coefficients λ, k and p^*.

If the value $\xi=0$ is introduced into Eqs. (3.12)–(3.15), the solution of the linear problem is obtained. This solution was presented in the paper [9]. If the value $p^*=0$ is put into Eqs. (3.12)–(3.15) the respective formulae for the case of a shell under pure shear are obtained. If, however, the value $s^*=0$ is inserted in the same equations, the respective formulae for the case of a shell under unidirectional compression are obtained.

The solution of the system of equations (3.12)–(3.15) in the full form permits to analyse the influence of the coefficients: of the shell form λ and of the shell shallowness k on the upper and lower critical values of a shell loading for a concrete multilayered shell at symmetrical structure, consisting of orthotropic layers. These upper and lower critical values of shell loadings are also expressed by the dimensionless coefficients p^*_u and p^*_l, and also s^*_u and s^*_l, respectively.

4. Numerical example and conclusions

As an example of applications the five-layered shell, shown in Fig. 4, is considered. The main directions of orthotropy of all shell layers are parallel to the axes x and y of the accepted coordinates system.

Young's moduli E_x and E_y, Poisson's ratios ν_x and ν_y, in the x and y directions, and also the shear moduli G_{xy} in surfaces, parallel to the $x-y$ surface, are put together in Table 1, in turn for each layer of a shell.

On the ground of Eqs. (3.12)–(3.15) for settled values of the compressive loading coefficient p^*, the adequate values of the shear loading coefficient s^* are determined as functions of the deflection coefficient ξ for different values of the coefficients k and λ. These relations in the form of some diagrams are presented and are shown in the successive Figures 5–14.

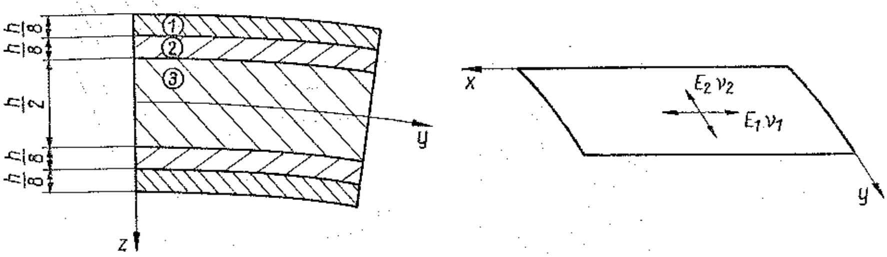

FIG. 4.

Detailed calculations for cases when $k=0$, $k=12$ and $k=24$ as well as $\lambda=0.5$, $\lambda=1.0$, $\lambda=1.5$ and $\lambda=2.0$ were performed on the ODRA–1204 computer.

Table 1. Assumed elastic constants of materials of separate shell layers

Layer	E_x	E_y	G_{xy}	ν_x	$\nu_y=\nu_x \frac{E_y}{E_x}$
1 and 5	$2E$	$1.4E$	$0.62E$	0.40	0.28
2 and 4	$1.5E$	$1.3E$	$0.53E$	0.35	0.30
3	E	$1.2E$	$0.42E$	0.30	0.36

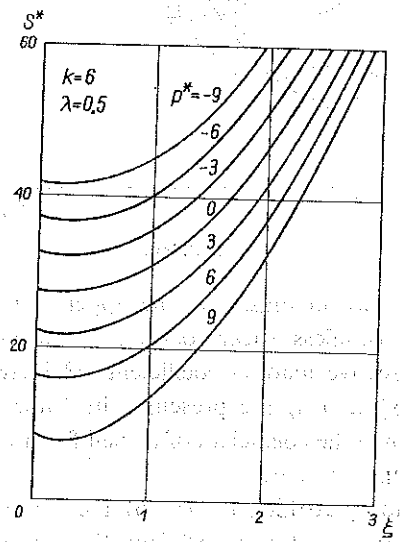

FIG. 5.

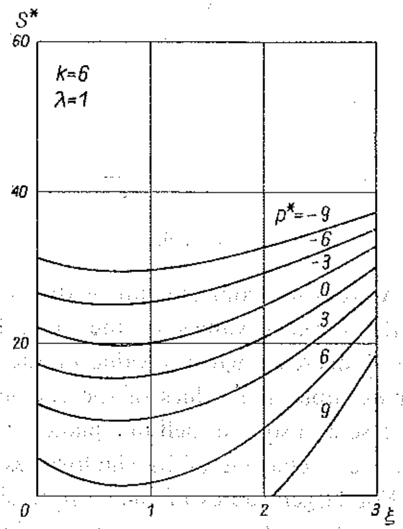

FIG. 6.

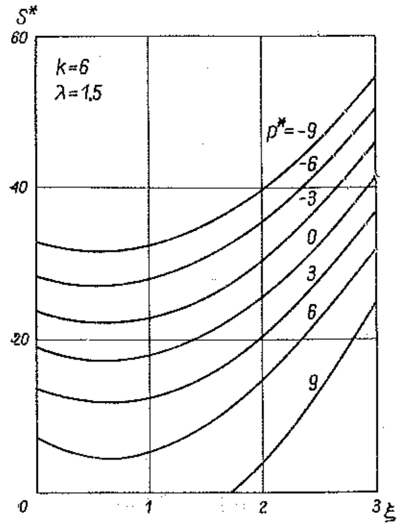

FIG. 7.

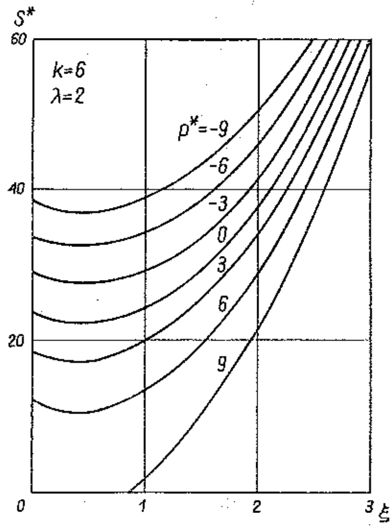

FIG. 8.

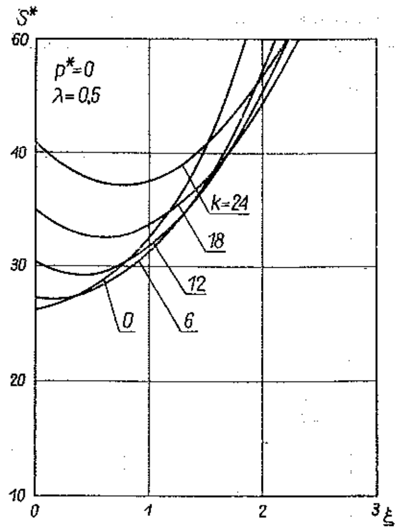

FIG. 9.

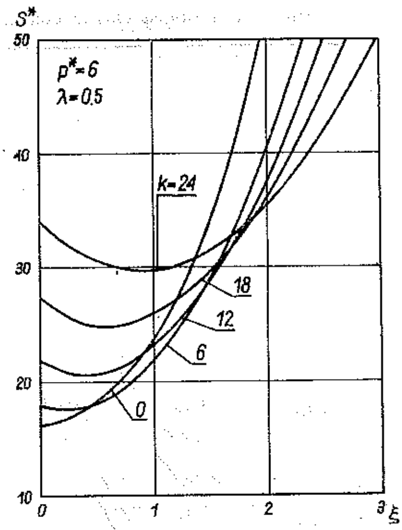

FIG. 10.

As follows from the run of the curves shown in Figs. 5–8, the upper — as well as the lower — values of the critical dimensionless shear loading coefficients s_u^* and s_l^* decrease when a value of the compressive loading coefficient p^* increases. For example, the values of the coefficients s_u^* and s_l^* are presented in Table 2 for the case of a square shell in a plane; this is when the coefficient of a shell form $\lambda=1.0$ and the coefficient of its shallowness amounts to $k=6$.

For larger values of the compressive loading coefficient ($p^*>6$) the extrema of the function $s^*=s^*(\xi)$ vanish and, in the considered range of deflections, the shell is in a constant equilibrium (Figs. 6, 7 and 8).

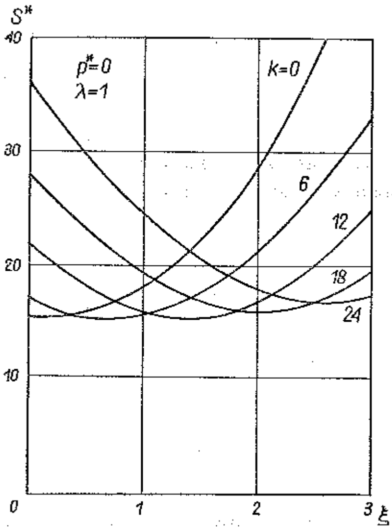

Fig. 11.

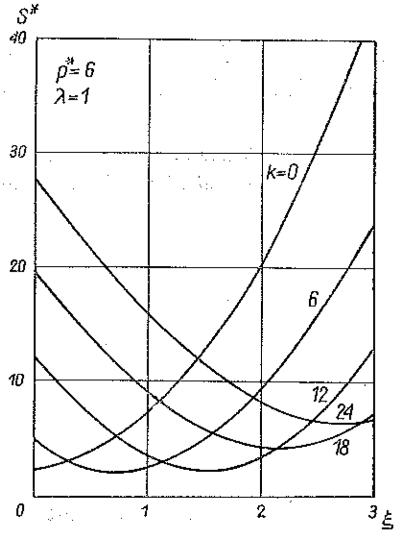

Fig. 12.

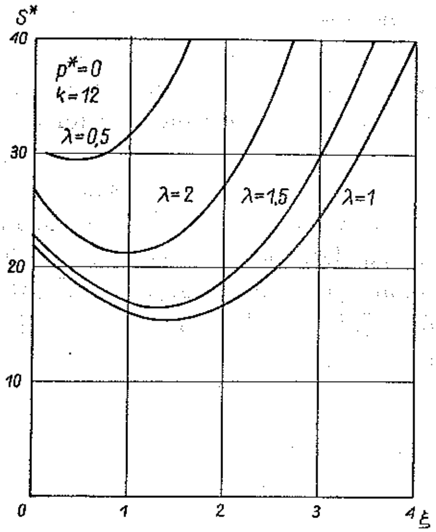

Fig. 13.

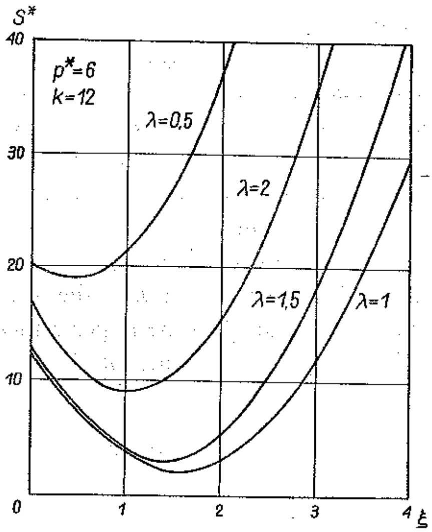

Fig. 14.

Table 2. Upper critical and lower critical values of the shear dimensionless coefficient s_u^* and s_l^* for a shell at the form coefficient $\lambda=1.0$ and at the shallowness coefficient $k=6$

p^*	s_u^*	s_l^*
0	17.32	15.35
3	12.08	9.87
6	5.18	2.20
decrease of values about:	55%	85%

Next, in Table 3 are presented the lower critical values of the shear loading coefficient $s_{l_1}^*$ for different values of the coefficients λ and k for the settled value of the compressive loading coefficient $p^*=3$.

Table 3. Lower critical values of the shear loading coefficient s_l^* for the value of the compressive loading coefficient $p^*=3$

k \ λ	0.5	1.0	1.5	2.0
0	20.91	9.93	11.86	17.16
12	24.30	9.92	10.89	15.79
24	32.56	11.70	9.58	12.35

From the data gathered in Table 3 it results that the values of the dimensionless coefficient s_l^* increase with an increase of the shell shallowness coefficient k when the shell form coefficient $\lambda=0.5$ and $\lambda=1.0$ but decrease for lengthened shells in the direction of cylinder generating lines ($\lambda=1.5$ and $\lambda=2.0$).

However, from the diagrams shown in Figs. 9–12, it can be seen that the upper critical values of the shear loading coefficient s_u^* always increase with an increase of the values of the shell shallowness coefficient k. This is also the case for each other value of the shell form coefficient λ. The increase of the coefficient s_u^* is the greatest for the square shell in a plane; this is when the shell form coefficient $\lambda=1.0$. As can be seen from the diagrams, shown examplarly for $k=12$ in Figs. 13 and 14, the values of the coefficients s_u^* and s_l^* are the smallest for the same value of the coefficient λ, i.e. when $\lambda=1.0$. In the next tables are gathered the ratio values of the lower critical value s_l^* to the upper critical value s_u^*, i.e. s_l^*/s_u^* of the shear loading coefficient for various values of the coefficients p^*, λ and k.

Table 4. The ratio values $\frac{s_l^*}{s_u^*}$ or various values of the compressive loading coefficient p^* for a shell at the shallowness coefficient $k=6$

p^* \ λ	0.5	1.0	1.5	2.0
0	0.99	0.89	0.90	0.93
3	0.98	0.81	0.84	0.87
6	0.97	0.43	0.58	0.82

As follows from the numerical data gathered in the above table, when the values of the compressive loading coefficient p^* increase, the values of the ratio s_l^*/s_u^* decrease for each value of the coefficient λ of the shell form. The decrease of value of this ratio is the greatest for the value $\lambda=1$. The smallest value of the ratio s_l^*/s_u^* also occurs for this value of the shell form coefficient λ.

As follows from the numerical data gathered in Table 5, the value of the ratio s_l^*/s_u^* decreases with an increase of the shell shallowness determined by the dimensionless coefficient k.

Table 5. Values of the ratio $\frac{s_l^*}{s_u^*}$ for various values of the compressive loading coefficients p^* for the square shell in a plane ($\lambda=1$)

p^* \ k	12	24
0	0.70	0.46
3	0.58	0.35
6	0.16	0.24

Numerical computations made for a similar but three-layered orthotropic shell of a symmetrical structure made it possible to reach similar conclusions as in the case considered above.

References

1. С. А. Амбарцумян, *Общая теория анизотропных оболочек*, Наука, Москва 1974.
2. А. С. Вольмир, *Устойчивость деформируемых систем*, Наука, Москва 1976.
3. Э. И. Григолюк, П. П. Чулков, *Нелинейные уравнения пологих многослойных оболочек регулярного строения*, Инж. журнал Механика твердого тела, 1. 1967.
4. А. М. Куршин, *Некоторые вопросы изгиба и устойчивости трехслойных цилиндрических оболочек*, Дисс. Ин-та Механики АН СССР, 1958.
5. О. Н. Ленько, *Устойчивость круговой цилиндрической ортотропной оболочки*, Расчет пространств. конструкции, 4, 1956.
6. W. Szyc, *Nieliniowe zagadnienie stateczności sprężystej trójwarstwowej otwartej powłoki walcowej*, Rozpr. Inżyn., 4, 1971.
7. T. Niezgodziński, *Stateczność wielowarstwowej powłoki w postaci wycinka walca, poddanej ścinaniu*, Zesz. Nauk. Politech. Łódz., Mechanika, 40, 1973, 45, 1976.
8. C. W. Bert, W. C. Crisman, G. M. Nordby, *Buckling of cylindrical and conical sandwich shells with orthotropic facings*, AJAA J., 7, 2, Feb. 1969.
9. N. X. Luu, *Liniowe zagadnienie utraty stateczności ścinanej wielowarstwowej powłoki w kształcie wycinka walca przy jednoczesnym ściskaniu wzdłuż tworzącej*, Zesz. Nauk. Politech. Łódz., Mechanika, 223, 44, 1976.

Streszczenie

STAN NADKRYTYCZNY WIELOWARSTWOWEJ POWŁOKI WALCOWEJ POD DZIAŁANIEM ŚCISKANIA I ŚCINANIA

W pracy przedstawiono wyniki teoretycznej analizy stanu nadkrytycznego cienkościennej, sprężystej powłoki wielowarstwowej o postaci wycinka walca, poddanej działaniu jednokierunkowego ściskania i jednoczesnego ścinania. Przyjęto, że powłoka jest zbudowana z warstw ortotropowych i ma budowę symetryczną.

Zagadnienie rozwiązano w sposób przybliżony na podstawie nieliniowej wersji teorii powłok anizotropowych, podanej przez S. A. Ambarcumiana.

Szczegółowe obliczenia numeryczne przeprowadzono przykładowo dla pięciowarstwowej powłoki, zbudowanej z warstw ortotropowych, a ich wyniki przedstawiono w postaci szeregu wykresów. Obliczenia te wykonano na komputerze ODRA-1204.

Резюме

ЗАКРИТИЧЕСКОЕ СОСТОЯНИЕ МНОГОСЛОЙНОЙ ОБОЛОЧКИ В ВИДЕ СЕКТОРА ЦИЛИНДРА ПОД ДЕЙСТВИЕМ СЖАТИЯ И СДВИГА

В работе представлены результаты теоретического анализа закритического состояния тонкостенной, упругой многослойной оболочки, в виде сектора цилиндра, подвергнутой действию однонаправленного сжатия и одновременного сдвига. Принимается, что оболочка построена из ортотропных слоев имеет симметричное строение. Задача решена приближенным образом на основе нелинейного варианта теории анизотропных оболочек приведенного С. А. Амбарцумяном.

Детальные численные расчеты примерно проведены для пятислойной оболочки, построенной из ортотропных слоев, а их результаты представлены в виде ряда графиков. Эти расчеты проведены на ЭЦВМ ОДРА-1204.

TECHNICAL UNIVERSITY OF ŁÓDŹ
INSTITUTE OF APPLIED MECHANICS

Received October 11, 1976.